

COMPOSITE ANTI-DISTURBANCE SWITCHED \mathcal{H}_2 CONTROL DESIGN FOR SWITCHED SYSTEMS

Emre KEMER*, Hasan BAŞAK**

*Engineering and Natural sciences, Electrical-Electronics Engineering, Uşak University, Uşak, Turkey

** Engineering, Electrical-Electronics Engineering, Artvin Çoruh University, Artvin, Turkey

emre.kemer@usak.edu.tr, hasanbasak@artvin.edu.tr

received 04 July 2024, revised 09 October 2024, accepted 10 October 2024

Abstract: This article addresses the challenge of integrated switched H_2 control with disturbance rejection capabilities for switched systems, particularly when external disturbances are present. A novel anti-disturbance switched H_2 control strategy is formulated, leveraging estimated disturbance values. The formulation is given in Linear Matrix Inequalities (LMIs), establishing sufficient conditions to ensure H_2 performance while maintaining closed-loop stability. To validate the effectiveness of the proposed methodology, it is applied to a practical aero-engine model. Through simulations, it is demonstrated that the closed-loop aero-engine model exhibits remarkable transient performance even in the face of external disturbances. These results underscore the efficacy of the developed approach in enhancing the robustness and performance of switched systems subjected to disturbances. The integration of anti-disturbance capabilities within the H_2 control framework offers a promising avenue for addressing real-world control challenges, particularly in systems characterized by switching dynamics and external perturbations.

Key words: composite anti-disturbance control, switched systems, dwell time, \mathcal{H}_2 -switched control, aero-engine model

1. INTRODUCTION

There are several system disturbances, which can lead to instability or poor performance. Therefore, several anti-disturbance control techniques have been developed by researchers to enhance the anti-disturbance performance of systems. For example, [1] developed a H_∞ control with an observer for eliminating a norm-bounded disturbance and a disturbance defined by an exogenous system on an aircraft model. [2] proposed a methodology for Markovian jump systems under the influence of multiple disturbances. A sliding mode observer and a feedback control law based on the backstepping method were employed in [3] for flexible spacecraft systems. [4] designed a flight controller for a helicopter system using a disturbance observer and a backstepping controller. A disturbance rejection control method was proposed by [5] using H_∞ control and the equivalent input disturbance method for an aircraft system. The equivalent input disturbance method was employed in [6] to estimate exogenous perturbations with the Lyapunov-based state feedback control law and in [7], authors improved the disturbance estimation performance of modelling equivalent input perturbations for a missile autopilot design. [8] developed a sliding mode controller in conjunction with a disturbance observer for a quadrotor helicopter where the disturbance observer estimates the impact of persistent and gradually changing disturbances. [9] suggested a methodology combining a sliding mode controller and a dual disturbance observer to manage spacecraft position and attitude dynamics, where the dual disturbance observer based controller attenuates both the external disturbances characterized by the exogenous model and the bounded disturbances. The helicopter slung load system was governed by a composite anti-disturbance model reference controller, which ensured asymptotic stability and L_2 –

L_∞ performance in [10]. A composite control strategy comprising a disturbance observer and a robust controller was designed by [11] to handle with multiple disturbances in a rigid spacecraft system, aiming to achieve anti-disturbance performance. A hybrid control approach was presented in [12] for Markovian jump systems affected by multiple disturbances. This approach specifically addresses an energy-bounded disturbance alongside an event-triggered sinusoidal disturbance characterized by unknown frequencies and amplitudes. An anti-disturbance control was designed in [13] which tackles the challenges of finite-time boundedness and disturbance rejection in takagi-sugeno fuzzy networked systems, particularly those susceptible to actuator faults, linear fractional uncertainties, and multiple disturbances. In [14], researchers investigate a distributed extended state observer design and a dual-side dynamic event-triggered output feedback anti-disturbance control strategy for interconnected systems facing quantization issues and multi-source disturbances.

In another research domain, there has been a notable rise in interest regarding the analysis of stability and design of controllers for switched systems [15], because switched systems find wide-ranging applications across various industries, including but not limited to the automotive industry, aviation, air traffic control systems, switching power converters, and so on [16]. At present, numerous significant findings have emerged regarding the stability and control synthesis of switched systems. Generally, the most prevalent approaches to designing switching laws involve state- and time-dependent switching rules [17,18,19]. A state-dependent switching law refers to a switching function that depends on the system state. Even though individual subsystems exhibit instability, the overall stability of the switched system can be preserved. Nevertheless, the chattering phenomenon [20] may be revealed because any

dwelt-time constraint cannot be guaranteed between switching instants. A few examples of dwelt-time switching laws [21, 22, 23] which are formulated based on time-dependent rules. The amplitude changes in switching controllers may lead to control bumps, negatively affecting transient performance and potentially causing instability. This issue was addressed in [24,25], where the authors proposed an H_∞ bumpless transfer controller specifically designed for switched interval type-2 (IT2) fuzzy systems. A fault tolerance and anti-disturbance attenuation using a two-dimensional modified repetitive control system was investigated in [26] for switched fuzzy systems with multiple disturbances.

Various disturbances occur during flight, which can significantly impact the performance of aero-engine systems. Consequently, developing anti-disturbance controllers for these systems is imperative. However, the challenge of implementing effective disturbance-rejection control in aero-engine systems especially in the presence of multiple disturbances remains largely unaddressed. This gap in the existing literature serves as the main motivation behind our study. By focusing on the unique challenges faced by aero-engine systems, we aim to contribute a robust framework for designing anti-disturbance controllers that can effectively manage multiple disturbances. Our research not only addresses this critical need but also provides innovative solutions that enhance the stability and performance of aero-engine systems in dynamic flight conditions. This work lays the groundwork for future advancements in control strategies within the aerospace industry, promoting greater safety and efficiency in aircraft operations. In this paper, we address the challenge of composite disturbance-rejection \mathcal{H}_2 control for switched systems. Many control systems encounter significant challenges from external disturbances that can compromise operational stability. Traditional control strategies often struggle to maintain performance under such conditions, leading to increased instability and inefficiency. To address these issues, developing an anti-disturbance approach is essential for ensuring consistent performance and reliability. The anti-disturbance switched \mathcal{H}_2 control method specifically enhances system performance and optimizes operational efficiency. We propose a composite anti-disturbance control scheme to effectively manage multiple disturbances. The need for effective control of time-varying systems, particularly those subjected to external disturbances, has led to the development of advanced control strategies. In this context, our composite anti-disturbance control approach integrates disturbance observer-based control with robust switching strategies, offering superior disturbance rejection compared to traditional methods. A key advantage of our method is the use of a state-dependent switching law, which makes the system highly adaptable to time-varying dynamics—a significant improvement over static or less adaptive control schemes. Additionally, the integration of an \mathcal{H}_2 based controller ensures optimal tracking performance. When combined with the disturbance observer, it outperforms standard \mathcal{H}_2 methods, providing better tracking accuracy while maintaining comparable levels of robustness. The proposed design also tackles common challenges in switching systems by carefully managing dwell times and switching conditions, ensuring both stability and high performance without typical drawbacks like chattering. The key contributions of this work are as follows: We propose a disturbance observer-based control approach and a switched state feedback \mathcal{H}_2 control method for a class of switched systems experiencing multiple disturbances. Here, the disturbance observer is designed to estimate the external disturbances described by an exogenous system. The outputs of the disturbance observer and the switched \mathcal{H}_2 state feedback controller are integrated to form a composite anti-disturbance switched

controller. We present conditions, formulated as LMIs, that guarantee robust stability of the closed-loop system while maintaining the specified \mathcal{H}_2 -norm. A growing number of articles has focused on control problems in aero-engine systems, highlighting the significance of this area in engineering. To demonstrate the effectiveness of our proposed composite anti-disturbance control scheme, we apply it to an aero-engine system. We achieve stability of the controlled aero-engine system by applying minimum dwell-time theory.

The structure of this paper is as follows: In the subsequent section, we provide the preliminaries and problem formulation. We then detail a composite anti-disturbance \mathcal{H}_2 control scheme using LMIs in Section 3. Application of the proposed control approach to an aero-engine model is detailed in Section 4. Following this, simulation results are presented in the subsequent section to show the effectiveness of the developed control scheme. Lastly, the conclusions of this paper are given.

Notation: The function $Tr(\cdot)$ represents the trace operation for square matrices. $He\{A\} = A + A'$ is called $He\{\cdot\}$. P are symmetric matrices and $P > 0$ (≥ 0) indicates positive definiteness (semi-definiteness). A symmetric matrix of the form $\begin{bmatrix} P & Q \\ Q' & P \end{bmatrix}$ is denoted as $\begin{bmatrix} P & Q \\ * & P \end{bmatrix}$. We denote \mathbb{R}^n as the n -dimensional Euclidean space and $\mathbb{R}^{p \times q}$ as the set of all $p \times q$ real matrices. Additionally, \mathbb{N} denotes the set of natural numbers.

2. PRELIMINARIES AND PROBLEM FORMULATION

Consider a dynamic system described by:

$$\frac{dx(\theta)}{d\theta} = A(\theta)x(\theta) + B(\theta)(\delta_1(\theta) + u(\theta)) + B_w(\theta)\delta_2(\theta) \quad (1)$$

in which the state denoted by $x(\theta)$ belongs to the n -dimensional real space, \mathbb{R}^n , the control signal represented as $u(\theta)$ resides in the k -dimensional real space, \mathbb{R}^k . External disturbances are an unknown disturbance, $\delta_2(\theta) \in \mathbb{R}^l$ and the disturbance, $\delta_1(\theta) \in \mathbb{R}^m$ generated by the following system:

$$\begin{aligned} \dot{w}(\theta) &= E(\theta)w(\theta) + F(\theta)\delta_3(\theta) \\ \delta_1(\theta) &= G(\theta)w(\theta) \end{aligned} \quad (2)$$

in which the state of the external disturbance system is $w(\theta) \in \mathbb{R}^p$ and the perturbations and uncertainties of the exogenous system are denoted by $\delta_3(\theta) \in \mathbb{R}^r$.

In this paper, the disturbance observer is formulated as:

$$\begin{aligned} \dot{\hat{v}}(\theta) &= (E(\theta) + LB(\theta)G(\theta))\hat{w}(\theta) + L(A(\theta)x(\theta) + B(\theta)u(\theta)) \\ \hat{w}(\theta) &= v(\theta) - Lx(\theta) \\ \hat{\delta}_1(\theta) &= G(\theta)\hat{w}(\theta) \end{aligned} \quad (3)$$

where $L \in \mathbb{R}^{p \times n}$ is the disturbance observer gain. In the composite disturbance observer-based control scheme, the state feedback controller is defined here with the form

$$u(\theta) = Kx(\theta) - \hat{\delta}_1(\theta) \quad (4)$$

where $\hat{\delta}_1$ signifies the estimated external disturbance and $K \in \mathbb{R}^{k \times n}$ is the controller. Also, it is assumed that all system states are accessible for measurement.

The disturbance estimation error can be calculated as

$$e_w(\theta) = w(\theta) - \widehat{w}(\theta) \quad (5)$$

Combining (2), (3) and (5), we have

$$\begin{aligned} \dot{e}_w(\theta) &= (E(\theta) + LB(\theta)G(\theta))e_w(\theta) + LB_w(\theta)\delta_2(\theta) \\ &+ F(\theta)\delta_3(\theta) \end{aligned} \quad (6)$$

Thus, the output is given such:

$$z(\theta) = C_1x(\theta) + C_2e_w(\theta) \quad (7)$$

Therefore, using (6) and (7) with (1) the augmented system is obtained

$$\begin{aligned} \dot{\tilde{x}}(\theta) &= \tilde{A}(\theta)\tilde{x}(\theta) + \tilde{B}(\theta)\delta(\theta) \\ z(\theta) &= \tilde{C}\tilde{x}(\theta) \end{aligned} \quad (8)$$

where

$$\begin{aligned} \tilde{x}(\theta) &= [x'(\theta), e'(\theta)]', \delta(\theta) = [\delta_2'(\theta), \delta_3'(\theta)]' \\ \tilde{A}(\theta) &= \begin{bmatrix} A(\theta) + B(\theta)K & B(\theta)G(\theta) \\ 0 & E(\theta) + LB(\theta)G(\theta) \end{bmatrix}, \\ \tilde{B}_w(\theta) &= \begin{bmatrix} B_w(\theta) & 0 \\ LB_w(\theta) & F(\theta) \end{bmatrix}, \\ \tilde{C} &= [C_1 \quad C_2]. \end{aligned}$$

2.1. Switched System Case

A nominal linear switching system emerges as a special case of system (1),

$$\begin{aligned} \frac{dx(\theta)}{d\theta} &= A_{\xi(\theta)}(\theta)x(\theta) + B_{\xi(\theta)}(\theta)(u(\theta) + \delta_1(\theta)) \\ &+ B_{w,\xi(\theta)}(\theta)\delta_2(\theta), \end{aligned} \quad (9)$$

where the switching rule function $\xi(\theta)$ defined for $\theta \geq 0$. $\xi(\theta)$ takes values from $1, \dots, M$, here M is the time-varying subsystems' number. Assuming that the system matrices of (9) are contained within the collective polytopes $\zeta_i(\theta)$ of the subsystems:

$$\zeta(\theta) = \bigcup_{i=1}^M \zeta_i(\theta) \quad (10)$$

where the definition of $\zeta_i(\theta)$ is as follows:

$$\zeta_i(\theta) = [A_i(\theta) \quad B_i(\theta) \quad B_{w,i}(\theta)] = \sum_{j=1}^N \kappa_j(\theta)\zeta_i^j, \quad (11)$$

where

$$\sum_{j=1}^N \kappa_j(\theta) = 1, \kappa_j(\theta) \geq 0, \theta \geq 0 \quad (12)$$

and

$$\zeta_i^j = [A_i^j \quad B_{u,i}^j \quad B_{w,i}^j] \quad (13)$$

Remark 1. In the preceding definition, the sub-polytopes are indexed by the variable i , which ranges from 1 to M . Additionally, j indexes the vertices of the corresponding sub-polytope, with each

sub-polytope assumed to possess N vertices. The convex combinations of these vertices give the matrices of the related sub-system. It is assumed that the sub-polytopes share some common regions and that the rates of change with respect to time for the polytopic coordinates $\kappa_j(\theta)$, $\forall j = 1, \dots, N$, are bounded.

Then, the external disturbance, $\delta_1(\theta)$ in (2) defined as:

$$\begin{aligned} \dot{w}(\theta) &= E_{\xi(\theta)}(\theta)w(\theta) + F_{\xi(\theta)}(\theta)\delta_3(\theta) \\ \delta_1(\theta) &= G_{\xi(\theta)}(\theta)w(\theta) \end{aligned} \quad (14)$$

Therefore, the disturbance observer is formulated such

$$\begin{aligned} \dot{\widehat{w}}(\theta) &= (E_{\xi(\theta)}(\theta) + L_{\xi(\theta)}B_{\xi(\theta)}(\theta)G_{\xi(\theta)}(\theta))\widehat{w}(\theta) \\ &- L_{\xi(\theta)}(A_{\xi(\theta)}(\theta)x(\theta) + B_{\xi(\theta)}(\theta)u(\theta)) \\ \widehat{w}(\theta) &= v(\theta) - L_{\xi(\theta)}x(\theta) \\ \widehat{\delta}_1(\theta) &= G_{\xi(\theta)}(\theta)\widehat{w}(\theta) \end{aligned} \quad (15)$$

and the state feedback control law is

$$u(\theta) = K_{\xi(\theta)}x(\theta) - \widehat{\delta}_1(\theta) \quad (16)$$

Combining (14), (15) and the disturbance estimation error $e_w(\theta) = w(\theta) - \widehat{w}(\theta)$, we have

$$\begin{aligned} \dot{e}_w(\theta) &= (E_{\xi(\theta)}(\theta) + L_{\xi(\theta)}B_{\xi(\theta)}(\theta)G_{\xi(\theta)}(\theta))e_w(\theta) \\ &+ L_{\xi(\theta)}B_{w,\xi(\theta)}(\theta)\delta_2(\theta) + F_{\xi(\theta)}(\theta)\delta_3(\theta) \end{aligned} \quad (17)$$

Finally, the augmented system is obtained based on the system in (9) and the system output

$$\begin{aligned} z(\theta) &= C_{1,\xi(\theta)}(\theta)x(\theta) + C_{2,\xi(\theta)}(\theta)e_w(\theta), \\ \dot{\tilde{x}}(\theta) &= \tilde{A}_{\xi(\theta)}\tilde{x}(\theta) + \tilde{B}_{\xi(\theta)}\delta(\theta) \\ z(\theta) &= \tilde{C}_{\xi(\theta)}\tilde{x}(\theta) \end{aligned} \quad (18)$$

where

$$\begin{aligned} \tilde{x}(\theta) &= [x'(\theta), e'(\theta)]', \delta(\theta) = [\delta_2'(\theta), \delta_3'(\theta)]' \\ \tilde{A}_{\xi(\theta)}(\theta) &= \begin{bmatrix} A_{\xi(\theta)}(\theta) + B_{\xi(\theta)}(\theta)K_{\xi(\theta)} & B_{\xi(\theta)}(\theta)G_{\xi(\theta)}(\theta) \\ 0 & E_{\xi(\theta)}(\theta) + L_{\xi(\theta)}B_{\xi(\theta)}(\theta)G_{\xi(\theta)}(\theta) \end{bmatrix}, \\ \tilde{B}_{w,\xi(\theta)}(\theta) &= \begin{bmatrix} B_{w,\xi(\theta)}(\theta) & 0 \\ L_{\xi(\theta)}B_{w,\xi(\theta)}(\theta) & F_{\xi(\theta)}(\theta) \end{bmatrix}, \\ \tilde{C}_{\xi(\theta)}(\theta) &= [C_{1,\xi(\theta)}(\theta) \quad C_{2,\xi(\theta)}(\theta)] \end{aligned}$$

The augmented system parameters are uncertain and presumed to reside in the union of the subsystems' polytopes as in (10). For simplicity, the notation θ will be dropped in the following sections.

Remark 2. In this paper, we employ a state-dependent switching law, as given in [18], which adheres to a dwell time constraint with a specified dwell time. This approach effectively manages the switching between different modes, thereby enhancing the overall stability and performance of the control system.

Definition 1. Throughout this paper, we adopt the assumption of a minimum dwell time constraint on the switching signal $\xi(\theta)$. This constraint implies that if the minimum dwell time is denoted by T , and the system's switching instants are represented as

$(\theta_1, \theta_2, \dots)$, then it holds that $\theta_{k+1} - \theta_k \geq T \forall k \geq 1$. Here, we define the time instants $\theta_{k,h} := \theta_k + hT/H$, where h ranges from 0 to H , and $\theta_{k,0} := \theta_k, \forall k$. Consequently, the minimum dwell time constraint T ensures that $\theta_{k,H} \leq \theta_{k+1,0}$. This definition is explained in Fig. 1.

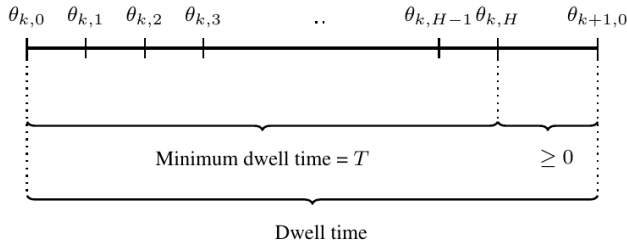


Fig. 1. Splitting the minimum dwell-time into H equal segments

3. COMPOSITE ANTI-DISTURBANCE CONTROL SCHEME

\mathcal{H}_2 control design is often adopted to deal with the transient performance of closed-loop systems. The \mathcal{H}_2 -norm in terms of LMIs can be defined as in the following lemma.

Lemma 1. (\mathcal{H}_2 -norm [27]) Given that A in the system (1) is Hurwitz and the corresponding transfer function is represented by $G(s) = C(sI - A)^{-1}B + D$, the following statements are equivalent:

\mathcal{H}_2 -norm of the system, $\|G\|_2^2 < \gamma^2$,

there exist symmetric matrices, $Y > 0$ and Z such that $Tr(Z) < \gamma^2$, $\begin{bmatrix} P & C' \\ * & Z \end{bmatrix} > 0$, $\begin{bmatrix} PA + A'P & PB \\ * & -I \end{bmatrix} < 0$.

Lemma 2. For the system (8), the following statements are equivalent to Lemma 1;

there exist symmetric matrices, $Q > 0, P > 0$ and Z such that

$$\begin{aligned} Tr(Z) < \gamma^2, \\ \begin{bmatrix} Q & 0 & QC'_1 \\ * & P & C'_2 \\ * & * & Z \end{bmatrix} > 0, \\ \begin{bmatrix} He\{A_c Q\} & BG & B_w & 0 \\ * & He\{PE_c\} & PLB_w & PF \\ * & * & -I & 0 \\ * & * & * & -I \end{bmatrix} < 0, \end{aligned}$$

Given positive scalars α and β , if there exist matrices X and Y , along with symmetric matrices $Q > 0, P > 0$, and Z , such that

$$\begin{aligned} Tr(Z) < \gamma^2, \\ \begin{bmatrix} Q & 0 & QC'_1 \\ * & P & C'_2 \\ * & * & Z \end{bmatrix} > 0, \\ \begin{bmatrix} He\{A_c Y\} & BG & B_w & 0 & \theta & 0 \\ * & He\{XE_c\} & XLB_w & XF & 0 & \Phi \\ * & * & -I & 0 & 0 & \beta(XLB_w)' \\ * & * & * & -I & 0 & \beta(XF)' \\ * & * & * & * & -\alpha(Y + Y') & 0 \\ * & * & * & * & * & -\beta(X + X') \end{bmatrix} < 0, \end{aligned}$$

where

$$A_c = A + BK, E_c = E + LBG, \theta = Q - Y' + \alpha A_c Y \text{ and } \Phi = P - X + \beta(XE_c)'$$

Proof: Denoting $P = \text{diag}(P_1, P_2)$ and replacing the system matrices in Lemma 1(ii) with the augmented system matrices (8), then the following equivalent conditions are obtained:

$$\begin{aligned} Tr(Z) < \gamma^2, \\ \begin{bmatrix} P_1 & 0 & C'_1 \\ * & P_2 & C'_2 \\ * & * & Z \end{bmatrix} > 0, \end{aligned} \tag{19}$$

$$\begin{bmatrix} He\{P_1 A_c\} & P_1 B G & P_1 B_w & 0 \\ * & He\{P_2 E_c\} & P_2 L B_w & P_2 F \\ * & * & -I & 0 \\ * & * & * & -I \end{bmatrix} < 0 \tag{20}$$

where

$$A_c = A + BK, E_c = E + LBG.$$

Denoting $\tilde{P} = \text{diag}(P_1^{-1}, I, I)$ and $\bar{P} = \text{diag}(P_1^{-1}, I, I, I)$, multiplying (19) and (20) by respectively \tilde{P} and \bar{P} from both sides, then the conditions in Lemma 2(ii) are obtained.

The proof of Lemma 2(ii) relies on applying the Finsler lemma in conjunction with Lemma 2(i). Also, multiplying Lemma 2(ii) the left by Y and from the right Y' the condition of Lemma 2(i) are obtained, where:

$$Y = \begin{bmatrix} I & 0 & 0 & 0 & A_c & 0 \\ 0 & I & 0 & 0 & 0 & E_c' \\ 0 & 0 & I & 0 & 0 & (LB_w)' \\ 0 & 0 & 0 & I & 0 & F' \end{bmatrix}$$

For the switched linear time-varying (LTV) system(18), the conditions in Lemma 2(i) can be rewritten as follows:

$$\begin{aligned} Tr(Z) < \gamma^2 \\ \begin{bmatrix} Q_i^j & 0 & Q_i^j (C_{1,i}^j)' \\ * & P_i^j & (C_{2,i}^j)' \\ * & * & Z \end{bmatrix} > 0 \\ \begin{bmatrix} -\dot{Q}_i^j + He\{A_c\} & B_i^j G_i^j & B_{w,i}^j & 0 \\ * & \dot{P}_i^j + He\{E_c\} & R_i^j B_{w,i}^j & P_i^j F_i^j \\ * & * & -I & 0 \\ * & * & * & -I \end{bmatrix} < 0 \end{aligned}$$

where $A_c = A_i^j Q_i^j + B_i^j S_i^j, E_c = P_i^j E_i^j + R_i^j B_i^j G_i^j$ and the matrices $P_i^j(\theta)$ and $Q_i^j(\theta)$ are assumed to be time-varying, hence the time derivative of $P_i^j(\theta)$ and $Q_i^j(\theta)$ are considered in the last condition. Also, it is assumed that the matrices $P_i(\theta)$ and $Q_i(\theta)$ can be expressed as convex combinations of the $P_i^j(\theta)$ and $Q_i^j(\theta)$, respectively.

As in [28], positive-definite Lyapunov matrices dependent on time and parameters, $Q_{\xi(\theta)}^j(\theta) \in \{Q_1^j(\theta), \dots, Q_M^j(\theta)\}$ and $P_{\xi(\theta)}^j(\theta) \in \{P_1^j(\theta), \dots, P_M^j(\theta)\}$, are defined as:

$$Q_i^j(\theta) = \begin{cases} Q_{i,h}^j + (Q_{i,h+1}^j - Q_{i,h}^j) \frac{\theta - \theta_{i,h}}{T/H} & \theta \in [\theta_{k,h}, \theta_{k,h+1}) \\ Q_{i,H}^j & \theta \in [\theta_{k,H}, \theta_{k+1}) \end{cases} \tag{21}$$

$$P_i^j(\theta) = \begin{cases} P_{i,h}^j + (P_{i,h+1}^j - P_{i,h}^j) \frac{\theta - \theta_{i,h}}{T/H} & \theta \in [\theta_{k,h}, \theta_{k,h+1}) \\ P_{i,H}^j & \theta \in [\theta_{k,H}, \theta_{k+1}) \end{cases} \tag{22}$$

Theorem 1. If a scalar $T > 0$ is given, and there exist matrices $S_{i,h}^j$, $R_{i,h}^j$, as well as positive-definite symmetric matrices Z , $P_{i,h}^j$, and $Q_{i,h}^j$ that satisfy the following LMIs minimization program $\forall i = 1, \dots, M$ and $j = 1, \dots, N$:

minimise $Tr(Z)$

subject to

$$\begin{bmatrix} Q_{i,h}^j & 0 & Q_{i,h}^j (C_{1,i}^j)' \\ * & P_{i,h}^j & (C_{2,i}^j)' \\ * & * & Z \end{bmatrix} > 0, \forall h \in \{0, \dots, H\},$$

$$\begin{bmatrix} \frac{Q_{i,h}^j - Q_{i,h+1}^j}{T/H} + He\{A_i^j Q_{i,h}^j + B_i^j S_{i,h}^j\} & B_i^j G_i^j & B_{w,i}^j & 0 \\ * & \frac{P_{i,h+1}^j - P_{i,h}^j}{T/H} + He\{P_{i,h}^j E_i^j + R_{i,h}^j B_i^j G_i^j\} & R_{i,h}^j B_{w,i}^j & P_{i,h}^j F_i^j \\ * & * & -I & 0 \\ * & * & * & -I \end{bmatrix} < 0, \quad (23a)$$

$$\begin{bmatrix} \frac{Q_{i,h}^j - Q_{i,h+1}^j}{T/H} + He\{A_i^j Q_{i,h+1}^j + B_i^j S_{i,h+1}^j\} & B_i^j G_i^j & B_{w,i}^j & 0 \\ * & \frac{P_{i,h+1}^j - P_{i,h}^j}{T/H} + He\{P_{i,h+1}^j E_i^j + R_{i,h+1}^j B_i^j G_i^j\} & R_{i,h+1}^j B_{w,i}^j & P_{i,h+1}^j F_i^j \\ * & * & -I & 0 \\ * & * & * & -I \end{bmatrix} < 0, \quad (23b)$$

where $h = 0, \dots, H - 1$,

$$\begin{bmatrix} He\{A_i^j Q_{i,H}^j + B_i^j S_{i,H}^j\} & B_i^j G_i^j & B_{w,i}^j & 0 \\ * & He\{P_{i,H}^j E_i^j + R_{i,H}^j B_i^j G_i^j\} & R_{i,H+1}^j B_{w,i}^j & P_{i,H+1}^j F_i^j \\ * & * & -I & 0 \\ * & * & * & -I \end{bmatrix} < 0, \quad (23c)$$

$$\begin{bmatrix} Q_{s,0}^j - Q_{i,H}^j & 0 \\ * & P_{i,H}^j - P_{s,0}^j \end{bmatrix} \geq 0, \forall s \in \{1, \dots, M\} \text{ and } s \neq i \quad (23d)$$

then gains of the switched state-feedback controller and the disturbance observer gains are computed as:

$$K_{\xi}^j(\theta) = \begin{cases} \left(S_{i,h}^j + (S_{i,h+1}^j - S_{i,h}^j) \frac{(\theta - \theta_{k,h})}{T/H} \right) \left(Q_{i,h}^j + (Q_{i,h+1}^j - Q_{i,h}^j) \frac{(\theta - \theta_{k,h})}{T/H} \right)^{-1}, & \theta \in [\theta_{k,h}, \theta_{k,h+1}), \\ \bar{S}_{i,H}^j \bar{Q}_{i,H}^j{}^{-1}, & \theta \in [\theta_{k,H}, \theta_{k+1}), \end{cases} \quad (24)$$

$$L_{\xi}^j(\theta) = \begin{cases} \left(P_{i,h}^j + (P_{i,h+1}^j - P_{i,h}^j) \frac{(\theta - \theta_{k,h})}{T/H} \right)^{-1} \left(R_{i,h}^j + (R_{i,h+1}^j - R_{i,h}^j) \frac{(\theta - \theta_{k,h})}{T/H} \right), & \theta \in [\theta_{k,h}, \theta_{k,h+1}), \\ \bar{P}_{i,H}^j{}^{-1} \bar{R}_{i,H}^j, & \theta \in [\theta_{k,H}, \theta_{k+1}), \end{cases} \quad (25)$$

Then it guarantees that the closed-loop system (18) exhibits global stability, while the closed-loop \mathcal{H}_2 -gain from d to z is maintained at $\sqrt{Tr(Z)}$ or less for any switching rule with a dwell-time equal to or greater than T .

Based on the above conditions and Lyapunov matrices, the following theorem is defined to provide solutions to the composite anti-disturbance control problem within the framework of the switched linear time-varying (LTV) system (18).

It is notable that prior to the initial switching event, the Lyapunov function experiences a decrease due to the conditions (23c). This indicates that the control strategy effectively preserves the Lyapunov function in the absence of switching, ensuring system stability and performance. Throughout the time span $\theta_k \leq \theta \leq \theta_k + T$, conditions (23a, 23b) derived from (21 and 22) ensure a consistent monotonous decrease in the Lyapunov function. Following this, conditions (23c) ensure the continuous decrease of $V(\theta, x)$ after $\theta_k + T$ and before the subsequent switching event. The non-increasing property of the Lyapunov function between any two arbitrary switching events is guaranteed by the conditions (23d).

Remark 3. According to Theorem 1, the state-feedback gains $K_i^j(\theta)$ and the disturbance observer gains $L_i^j(\theta)$ vary over time and depend on vertices. Nonetheless, these gains are often impractical for real-world use. Instead of those, time-invariant state-feedback gains and disturbance observer gains are often preferred. Therefore, the following theorem is formulated by using the conditions in Lemma 2(ii).

Remark 4. The computational complexity is given by $N(3MH + 3M - 1)$, where N represents the number of vertices, M is the number of subsystems, and H is the number of time instants. From this equation, we can conclude that both N and M contribute linearly to the overall computational complexity. This implies that if either the number of vertices or the number of subsystems increases, the computational effort will increase proportionately.

Theorem 2. For the given scalars $T > 0, \alpha > 0$, and $\beta > 0$, if there are matrices $S_{i,h}^j, R_{i,h}^j, X_{i,h}^j, Y_{i,h}^j$, and positive-definite symmetric matrices $Z, P_{i,h}^j$, and $Q_{i,h}^j; \forall i = 1, \dots, M$ and $j = 1, \dots, N$ that satisfy the following LMI minimization conditions:

minimise $Tr(Z)$
subject to

$$\begin{bmatrix} Q_{i,h}^j & 0 & Q_{i,h}^j(C_{1,i}^j)' \\ * & P_{i,h}^j & (C_{2,i}^j)' \\ * & * & Z \end{bmatrix} > 0, \forall h \in \{0, \dots, H\} \quad (26)$$

$$\begin{bmatrix} \Gamma_h & B_i^j G_i^j & B_{w,i}^j & 0 & Q_{i,h}^j - Y_{i,h}^j + \alpha(A_i^j Y_{i,h}^j + B_i^j S_{i,h}^j) & 0 \\ * & \vartheta_h & R_{i,h}^j B_{w,i}^j & X_{i,h}^j F_i^j & 0 & P_{i,h}^j - X_{i,h}^j + \beta(X_{i,h}^j E_i^j + R_{i,h}^j B_i^j G_i^j)' \\ * & * & -I & 0 & 0 & \beta(R_{i,h}^j B_{w,i}^j)' \\ * & * & * & -I & 0 & \beta(X_{i,h}^j F_i^j)' \\ * & * & * & * & -\alpha(S_{i,h}^j + S_{i,h}^j)' & 0 \\ * & * & * & * & * & -\beta(X_{i,h}^j + X_{i,h}^j)' \end{bmatrix} < 0, \quad (27a)$$

$$\begin{bmatrix} \Gamma_{h+1} & B_i^j G_i^j & B_{w,i}^j & 0 & Q_{i,h+1}^j - Y_{i,h+1}^j + \alpha(A_i^j Y_{i,h+1}^j + B_i^j S_{i,h+1}^j) & 0 \\ * & \vartheta_{h+1} & R_{i,h+1}^j B_{w,i}^j & P_{i,h+1}^j F_i^j & 0 & P_{i,h+1}^j - X_{i,h+1}^j + \beta(X_{i,h+1}^j E_i^j + R_{i,h+1}^j B_i^j G_i^j)' \\ * & * & -I & 0 & 0 & \beta(R_{i,h+1}^j B_{w,i}^j)' \\ * & * & * & -I & 0 & \beta(X_{i,h+1}^j F_i^j)' \\ * & * & * & * & -\alpha(S_{i,h+1}^j + S_{i,h+1}^j)' & 0 \\ * & * & * & * & * & -\beta(X_{i,h+1}^j + X_{i,h+1}^j)' \end{bmatrix} < 0, \quad (27b)$$

where

$h = 0, \dots, H - 1$ and

$$\Gamma_h = \frac{Q_{i,h}^j - Q_{i,h+1}^j}{T/H} + He\{A_i^j Y_{i,h}^j + B_i^j S_{i,h}^j\}, \quad \Gamma_{h+1} = \frac{Q_{i,h}^j - Q_{i,h+1}^j}{T/H} + He\{A_i^j Y_{i,h+1}^j + B_i^j S_{i,h+1}^j\},$$

$$\vartheta_h = \frac{P_{i,h+1}^j - P_{i,h}^j}{T/H} + He\{X_{i,h}^j E_i^j + R_{i,h}^j B_i^j G_i^j\}, \quad \vartheta_{h+1} = \frac{P_{i,h+1}^j - P_{i,h}^j}{T/H} + He\{X_{i,h+1}^j E_i^j + R_{i,h+1}^j B_i^j G_i^j\},$$

$$\begin{bmatrix} \Gamma_H & B_i^j G_i^j & B_{w,i}^j & 0 & Q_{i,H}^j - Y_{i,H}^j + \alpha(A_i^j Y_{i,H}^j + B_i^j S_{i,H}^j) & 0 \\ * & \vartheta_H & R_{i,H}^j B_{w,i}^j & X_{i,H}^j F_i^j & 0 & P_{i,H}^j - X_{i,H}^j + \beta(X_{i,H}^j E_i^j + R_{i,H}^j B_i^j G_i^j)' \\ * & * & -I & 0 & 0 & \beta(R_{i,H}^j B_{w,i}^j)' \\ * & * & * & -I & 0 & \beta(X_{i,H}^j F_i^j)' \\ * & * & * & * & -\alpha(S_{i,H}^j + S_{i,H}^j)' & 0 \\ * & * & * & * & * & -\beta(X_{i,H}^j + X_{i,H}^j)' \end{bmatrix} < 0, \quad (27c)$$

where

$$\Gamma_H = He\{A_i^j Y_{i,H}^j + B_i^j S_{i,H}^j\} \text{ and } \vartheta_H = He\{X_{i,H}^j E_i^j + R_{i,H}^j B_i^j G_i^j\},$$

$$\begin{bmatrix} Q_{s,0}^j - Q_{i,H}^j & 0 \\ * & P_{i,H}^j - P_{s,0}^j \end{bmatrix} \geq 0, \forall s \in \{1, \dots, M\} \text{ and } s \neq i \quad (27d)$$

then gains of the switched state-feedback controller and the disturbance observer gains are computed as:

$$K_{\xi}^j(\theta) = \begin{cases} (S_{i,h}^j + (S_{i,h+1}^j - S_{i,h}^j) \frac{(\theta - \theta_{k,h})}{T/H}) (Y_{i,h}^j + (Y_{i,h+1}^j - Y_{i,h}^j) \frac{(\theta - \theta_{k,h})}{T/H})^{-1}, & \theta \in [\theta_{k,h}, \theta_{k,h+1}), \\ \bar{S}_{i,H}^j \bar{Y}_{i,H}^j^{-1}, & \theta \in [\theta_{k,H}, \theta_{k+1}), \end{cases} \quad (28)$$

$$L_{\xi}^j(\theta) = \begin{cases} (X_{i,h}^j + (X_{i,h+1}^j - X_{i,h}^j) \frac{(\theta - \theta_{k,h})}{T/H})^{-1} (R_{i,h}^j + (R_{i,h+1}^j - R_{i,h}^j) \frac{(\theta - \theta_{k,h})}{T/H}), & \theta \in [\theta_{k,h}, \theta_{k,h+1}), \\ \bar{X}_{i,H}^j^{-1} \bar{R}_{i,H}^j, & \theta \in [\theta_{k,H}, \theta_{k+1}), \end{cases} \quad (29)$$

where, ensures that the closed-loop system (18) maintains global stability. Additionally, In scenarios where the dwell-time is T or greater, the closed-loop \mathcal{H}_2 -gain from d to z is limited to $\sqrt{Tr(Z)}$ or lower.

Remark 5. Theorem 2 provides vertex-dependent and time-varying state-feedback gains, $K_i^j(\theta)$, and disturbance observer gains, $L_i^j(\theta)$. However, if $S_{i,h}^j$, $Y_{i,h}^j$, $X_{i,h}^j$, and $R_{i,h}^j$ are selected independently of h and j , then these gains become time-invariant. They can be computed as $K_i = S_i Y_i^{-1}$ and $L_i = X_i^{-1} R_i$.

Remark 6. The \mathcal{H}_2 controller ensures optimal tracking performance by minimizing the quadratic cost function associated with tracking error and control effort. Integrating a disturbance observer enhances this performance by compensating for disturbances, improving tracking accuracy and overall system effectiveness. This combination allows the controller to adapt to varying disturbance levels, making it more versatile in handling unpredictable real-world scenarios.

It is important to note that as the size of the LMIs increases, there is a potential for a greater computational burden. Larger LMIs can introduce higher complexity in the numerical solving process, requiring more computational resources and time. However, advancements in modern computing technology have made it feasible to manage these challenges effectively. Furthermore, this computational complexity primarily arises during the initial design phase. Once the control strategies are established, the size of the LMIs becomes less significant, as they do not affect real-time implementation. Consequently, the initial investment in computational resources can yield robust and efficient control solutions that perform effectively in practice.

4. APPLICATION TO AERO-ENGINE MODEL

In this section, we showcase the implementation of the proposed anti-disturbance control scheme on the speed control system of the GE-90 aero-engine. We begin by presenting the GE-90 aero-engine model and then delve into the discussion of simulation results.

4.1. Aero-engine model

The aero-engine is comprised of essential components such as a combustion chamber, turbine, and compressor. Both the compressor and turbine feature high-pressure and low-pressure stages with rotating blades. The high-pressure compressor and turbine are concentrically aligned via a separate shaft, while the low-pressure compressor and turbine, along with the fan, rotate synchronously. Positioned at the inlet, the fan facilitates airflow, and a variable bleed valve is employed to extract gas from the core. Additionally, variable stator vanes aid in reducing flow separation within the compressor blades. Further details can be found in [29, 30]. The aero-engine has complex and highly non-linear dynamics. In the literature, different models of aero-engines have been developed. For this study we will use an LPV model of aero-engine (GE-90) which has been proposed by [29]. The altitude is normalized by 10000 and the fan speed by 3000. An LPV model of the uncertain state-space presentation is

$$\begin{bmatrix} \Delta \dot{N}_f \\ \Delta \dot{N}_c \\ B_w \delta_2 \end{bmatrix} = A(m, h, f) \begin{bmatrix} \Delta N_f \\ \Delta N_c \end{bmatrix} + B(m, h, f) (\Delta W_F + \delta_1) + \quad (30)$$

and the external disturbance system

$$\begin{aligned} \dot{w}(\theta) &= E_{\xi(\theta)} w(\theta) + F_{\xi(\theta)} \delta_3(\theta) \\ \delta_1(\theta) &= G_{\xi(\theta)} w(\theta) \end{aligned} \quad (31)$$

where m , h and f denote the Mach number, altitude and fan speed respectively. $\Delta N_f = N_f - N_{f0}$ is the fan speed increment, $\Delta N_c = N_c - N_{c0}$ is the core speed increment and $\Delta W_F = W_F - W_{F0}$ is the fuel flow increment. Also, δ_1 is the external disturbance, $\delta_2 = t e^{-t}$ is another disturbance and $\delta_3 = t e^{-t}$ is an additional disturbance which results from the perturbations and uncertainties in the external disturbance. The engine pressure ratio (EPR) increment is

$$EPR = C \begin{bmatrix} \Delta N_f \\ \Delta N_c \end{bmatrix}$$

Here, the Mach number, the altitude and the fan speed parameters vary between [0 - 0.84], [0 - 42000] and [1497 - 2432] respectively. Using these parameters, the system has been partitioned into four intersecting cells, as illustrated in Fig. 2. Model parameters can be obtained for each vertex and cell according to [23].

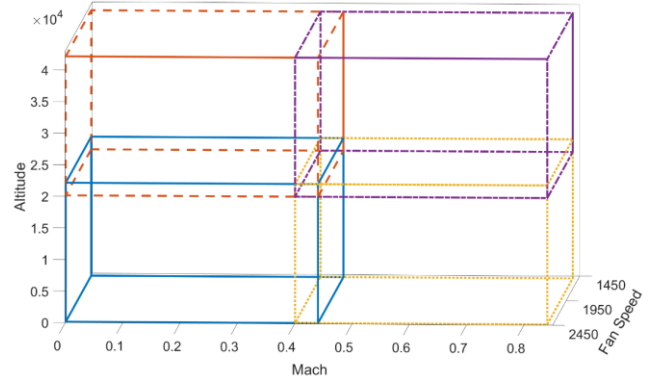


Fig. 2. The cell divisions of the parameters

Then, using LPV model in (30) with vertices of each cell, the switch system matrices A_i^j, B_i^j and C_i^j in (9) are obtained and the matrices $B_{w,i}^j, E_i^j, F_i^j, G_i^j$ and $C_{2,i}^j$ for $i \in \{1, \dots, 4\}$ and $j \in \{1, \dots, 8\}$ are given as:

$$\begin{aligned} B_{w,i}^j &= \begin{bmatrix} 0.1 \\ 0.2 \end{bmatrix}, & E_i^j &= \begin{bmatrix} 0 & -1 \\ 1 & 0 \end{bmatrix}, & F_i^j &= \begin{bmatrix} 0.002 \\ 0.001 \end{bmatrix}, \\ G_i^j &= \begin{bmatrix} 3 & 2 \end{bmatrix}, & C_{2,i}^j &= \begin{bmatrix} 0.1 & 1 \end{bmatrix} \end{aligned}$$

Then, solving Theorem 2 by using these matrices with the scalars $\alpha = \beta = 0.04$, $T = 0.1$ and $H = 1$, from equations (28) and (29), the gains of the switched controller and disturbance observer are computed as:

$$\begin{aligned} K_1 &= [0.0013 \quad -0.0064], & K_2 &= [-0.0633 \quad 0.0090] \\ K_3 &= [0.0034 \quad -0.0066], & K_4 &= [-0.0643 \quad 0.0085] \\ L_1 &= \begin{bmatrix} -0.0090 & -0.0043 \\ -0.0043 & -0.0025 \end{bmatrix}, & L_2 &= \begin{bmatrix} -0.0076 & -0.0036 \\ -0.0036 & -0.0022 \end{bmatrix} \\ L_3 &= \begin{bmatrix} -0.0090 & -0.0042 \\ -0.0042 & -0.0025 \end{bmatrix}, & L_4 &= \begin{bmatrix} -0.0064 & -0.0030 \\ -0.0030 & -0.0019 \end{bmatrix}. \end{aligned}$$

4.2. Simulation results and discussion

This section presents the simulation results of the proposed control scheme with the non-linear model of the GE-90 aero-engine. Initially, we adopt the non-linear validation model of the GE-90 aero-engine from [23] as:

$$\begin{aligned} \Delta \dot{N}_f &= -5.4452\Delta N_f - 3.1335\Delta N_f\Delta N_c + 5.1842\Delta N_f^2 \\ &\quad + 2.2142\Delta N_c + 0.2273\Delta N_c^2 + 230.6739\Delta W_F \\ &\quad - 86.2131\Delta N_f\Delta W_F + 25.0211\Delta N_c\Delta W_F \\ \Delta \dot{N}_c &= -0.1849\Delta N_f + 8.7942\Delta N_f\Delta N_c + 2.0938\Delta N_f^2 \\ &\quad - 7.0882\Delta N_c - 0.7456\Delta N_c^2 + 653.5547\Delta W_F \\ &\quad - 395.5347\Delta N_f\Delta W_F + 112.0966\Delta N_c\Delta W_F. \end{aligned}$$

To analyze the effectiveness of the proposed control approach, a standard H_2 controller is designed using the $h2syn$ function in the MATLAB Toolbox. Two scenarios were examined for the standard H_2 control approach. In the first scenario, the GE-90 aero-engine model was simulated using the standard H_2 control without a disturbance estimation. The fan speed and core speed are depicted in Fig. 3, while the EPR increment for the GE-90 aero-engine is shown in Fig. 4. It is evident that the standard H_2 control does not mitigate the disturbance effect. Next, the same model was simulated with the incorporation of the following disturbance observer:

$$L = \begin{bmatrix} -0.0090 & -0.0043 \\ -0.0043 & -0.0025 \end{bmatrix}$$

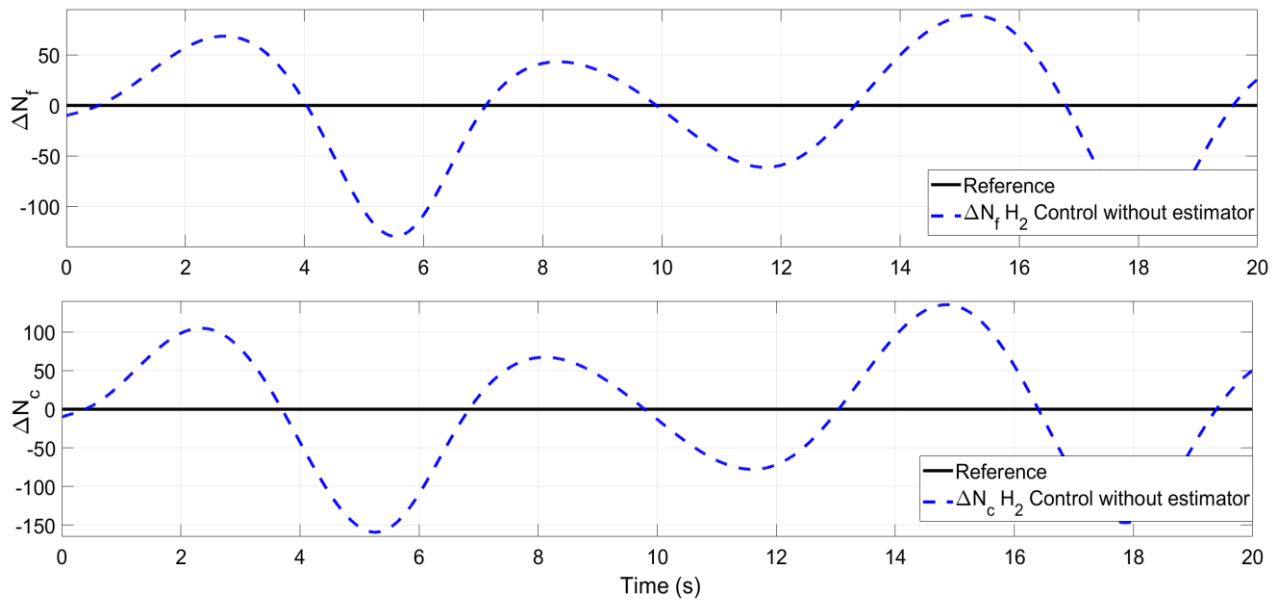


Fig. 3. The \mathcal{H}_2 control responses of the fan and core speed increments without an estimator

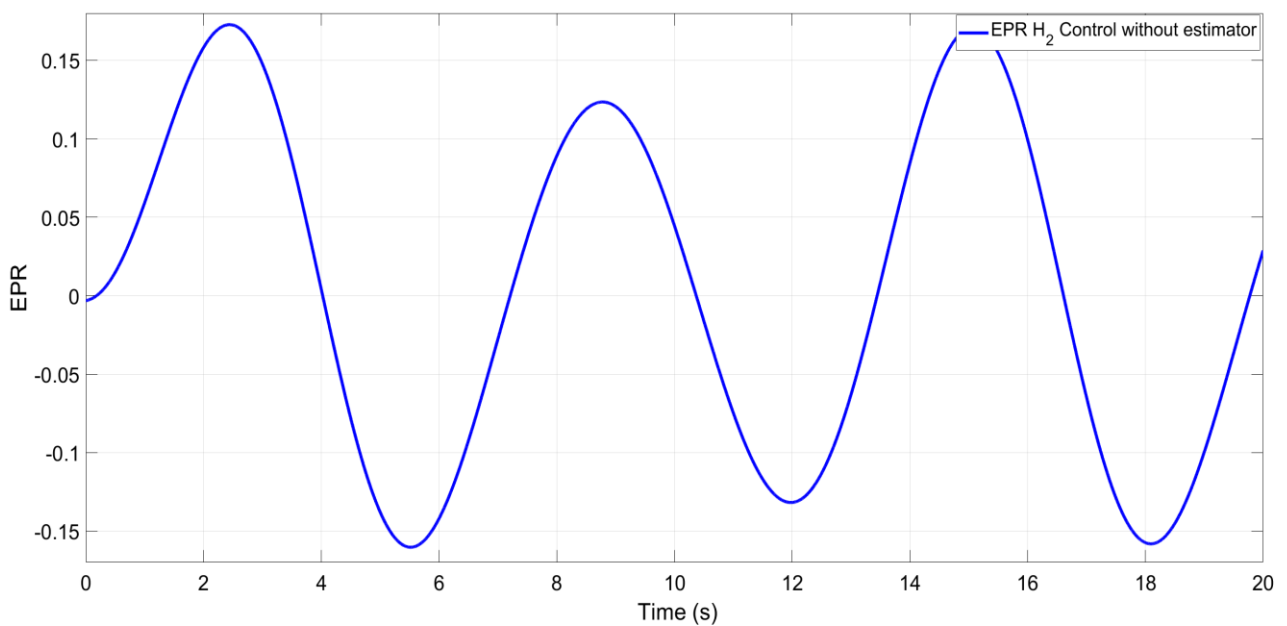


Fig. 4. \mathcal{H}_2 control response of the EPR increment without an estimator

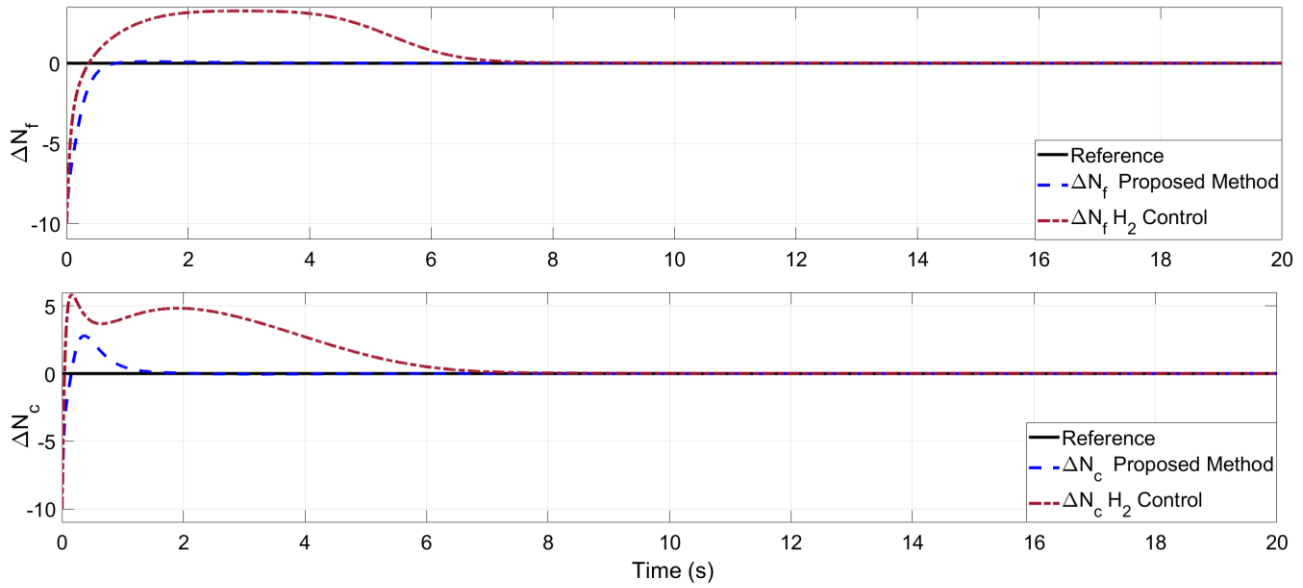


Fig. 5. The fan and core speed increments

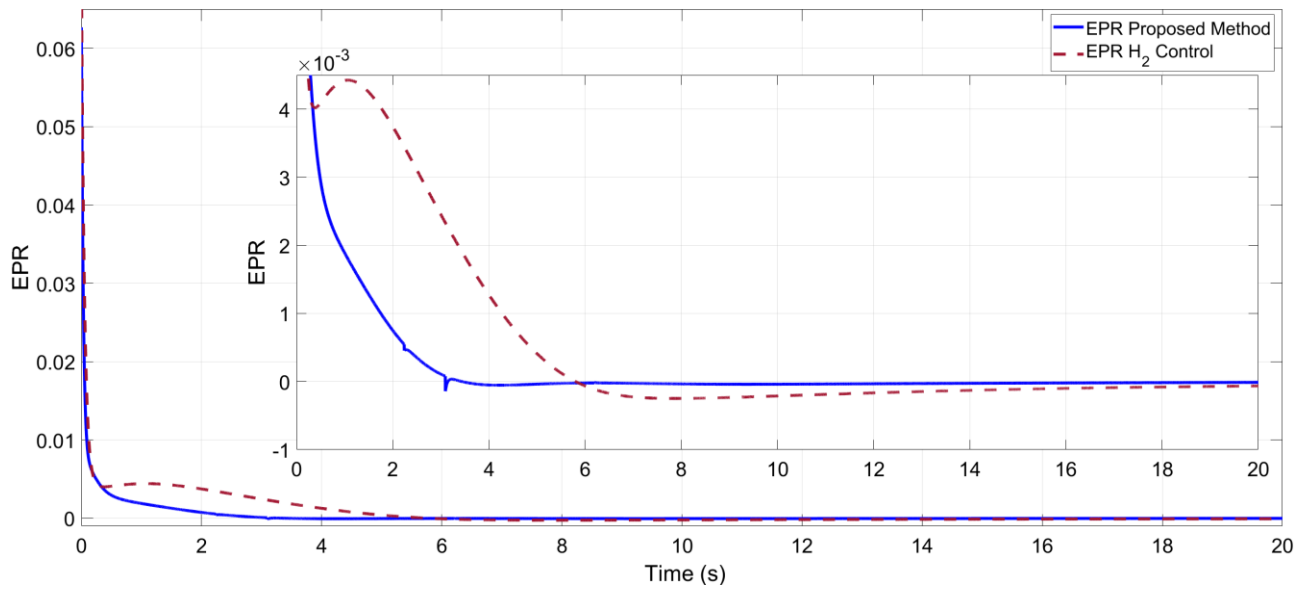


Fig. 6. EPR increment

Furthermore, we compare the simulation results of the proposed method and the standard H_2 controller with a disturbance observer. The responses of the fan speed and the core speed are presented in Fig. 5, while the EPR increment of the GE-90 aero-engine is depicted in Fig. 6. In addition, the comparison of the variation between the external disturbance and its estimation is illustrated in Fig. 7. The performance of the disturbance observer, showing that the estimated disturbance closely matches the actual disturbance profile. The system successfully maintains stability and performance, with settling times of $EPR = 3.5\text{ s}$, $\Delta N_c = 1.5\text{ s}$, and $\Delta N_f = 0.8\text{ s}$ using the proposed control structure. In comparison, under the standard H_2 control, the system exhibits settling times of $EPR = 20\text{ s}$, $\Delta N_c = 7\text{ s}$, and $\Delta N_f = 7\text{ s}$. This demonstrates the effectiveness of the observer in real-time disturbance estimation. Additionally, the switching function under the dwell-time is displayed in Fig. 8. Incorporating dwell time enhances

control performance by reducing energy fluctuations and ensuring system stability. By allowing brief pauses during the switching process, our method mitigates the oscillations typically associated with abrupt transitions, fostering a more stable operational environment. Notably, the time-varying nature of our approach facilitates smoother transitions, avoiding the harsh shifts that can destabilize the system. This smoothness not only improves overall responsiveness but also contributes to a more reliable control strategy, reinforcing the advantages of our proposed method compared to existing techniques. Overall, the simulation results confirm that the proposed anti-disturbance control scheme effectively eliminates the external disturbance given in (31) and stabilizes the nonlinear validation model of the GE-90 aero-engine.

5. CONCLUSION

This paper tackles the composite anti-disturbance switched control problem for switched systems. The dwell time approach has been used to analyze the robust stability with \mathcal{H}_2 -norm performance index using the linear matrix inequalities conditions. The gains of the switched \mathcal{H}_2 controller and the gain of the disturbance observer are computed by solving a convex LMI optimization problem. Then, the proposed control scheme is successfully implemented in an aero-engine model. A standard \mathcal{H}_2 controller method is used to analyse the efficiency of the proposed control approach. Simulation results validate the effectiveness of the proposed control scheme under the external disturbance. In future works, we will consider the disturbance suppression with input saturation problem in the application of aerospace systems.

REFERENCES

- Wei X, Guo L. Composite disturbance-observer-based control and H_∞ control for complex continuous models. *International Journal of Robust and Nonlinear Control: IFAC-Affiliated Journal*. 2010; 20(1): 106-118.
- Yao X, Guo L. Composite anti-disturbance control for Markovian jump nonlinear systems via disturbance observer. *Automatica*. 2013; 49(8): 2538-2545.
- Sun H, Hou L, Zong G, et al. Composite anti-disturbance attitude and vibration control for flexible spacecraft. *IET Control Theory & Applications*. 2017; 11(14): 2383-2390.
- Li Y, Chen M, Ge SS, et al. Anti-disturbance control for attitude and altitude systems of the helicopter under random disturbances. *Aerospace Science and Technology*. 2020; 96: 105561.
- Li T, Yang H, Tian J, et al. Improved disturbance rejection control based on H_∞ synthesis and equivalent-input-disturbance for aircraft longitudinal autopilot design. *Proceedings of the Institution of Mechanical Engineers, Part G: Journal of Aerospace Engineering*. 2018; 233(9): 3323-3335.
- Gao F, Wu M, She J, et al. Disturbance rejection in nonlinear systems based on equivalent-input-disturbance approach. *Applied Mathematics and Computation*. 2016; 282: 244-253.
- Li T, Zhang S, Yang H, et al. Robust missile longitudinal autopilot design based on equivalent-input-disturbance and generalized extended state observer approach. *Proceedings of the Institution of Mechanical Engineers, Part G: Journal of Aerospace Engineering*. 2016; 229(6): 1025-1042.
- Aboudonia A, Rashad R, El-Badawy A. Composite hierarchical anti-disturbance control of a quadrotor UAV in the presence of matched and mismatched disturbances. *Journal of Intelligent & Robotic Systems*. 2018; 90(1): 201-216.
- Zengbo L, Yukai Z, Jianzhong Q. Composite anti-disturbance position and attitude control for spacecraft with parametric uncertainty and flexible vibration. *Chinese Journal of Aeronautics*. 2022; 35(12): 242-252.
- Liu L, Chen M, Li T, et al. Composite Anti-Disturbance Reference Model $L_2 - L_\infty$ Control for Helicopter Slung Load System. *Journal of Intelligent & Robotic Systems*. 2021; 102(1): 1-21.
- Cao S, Guo L, Ding Z. Event-triggered anti-disturbance attitude control for rigid spacecrafts with multiple disturbances. *International Journal of Robust and Nonlinear Control*. 2021; 31(2): 344-357.
- Yao X, Wen X. Composite hierarchical hybrid anti-disturbance control for Markovian jump systems with event-triggered disturbance. *Systems & Control Letters*. 2024; 185: 105734.
- Sakthivel R, Elayabharath VT, Satheesh T, et al. Design of anti-disturbance reliable control for fuzzy networked control systems with multiple disturbances. *International Journal of Fuzzy Systems*. 2024; 26(1): 105-120.
- Sun H, Liu Y, Jiao T, et al. Distributed extended state observer design and dual-side dynamic event-triggered output feedback anti-disturbance control for nonlinear interconnected systems with quantization. *Journal of the Franklin Institute*. 2024; 106847.
- Lin H, Antsaklis PJ. Stability and stabilizability of switched linear systems: a survey of recent results. *IEEE Transactions on Automatic Control*. 2009; 54(2): 308-322.
- Liberzon D, Morse AS. Basic problems in stability and design of switched systems. *IEEE control systems magazine*. 1999; 19(5): 59-70.
- Geromel JC, Colaneri P. Stability and stabilization of continuous-time switched linear systems. *SIAM Journal on Control and Optimization*. 2006; 45(5): 1915-1930.
- Allerhand LI, Shaked U. Robust control of linear systems via switching. *IEEE Transactions on Automatic Control*. 2012; 58(2): 506-512.
- Liu F, Chen M, Li T. Resilient H_∞ control for uncertain turbofan linear switched systems with hybrid switching mechanism and disturbance observer. *Applied Mathematics and Computation*. 2022; 413: 126597.
- Deaecto GS, Souza M, Geromel JC. Chattering free control of continuous-time switched linear systems. *IET Control Theory & Applications*. 2014; 8(5): 348-354.
- Gershon E, Shaked U. Robust State-Dependent Switching of Linear Systems with Dwell Time. In *Advances in H_∞ Control Theory*. Springer Cham. 2019; 27-41.
- Wang J, Huang Z, Wu Z, et al. Extended dissipative control for singularly perturbed PDT switched systems and its application. *IEEE Transactions on Circuits and Systems I: Regular Papers*. 2020; 67(12): 5281-5289.
- Xiang W. Stabilization for continuous-time switched linear systems: A mixed switching scheme. *Nonlinear Analysis: Hybrid Systems*. 2020; 36: 100872.
- Zhang S, Zhao J. Dwell-Time-Dependent H_∞ Bumpless Transfer Control for Discrete-Time Switched Interval Type-2 Fuzzy Systems. *IEEE Transactions on Fuzzy Systems*. 2021; 30(70): 2426-2437.
- Zhang S, Zhao J. Membership-function-dependent H_∞ bumpless transfer control for switched interval type-2 fuzzy systems with time-delay. *Nonlinear Analysis: Hybrid Systems*. 2024; 52: 101457.
- Priyanka S, Sakthivel R, Mohanapriya S, et al. Composite fault-tolerant and anti-disturbance control for switched fuzzy stochastic systems. *ISA transactions*. 2022; 125: 99-109.
- Scherer C, Weiland S. Linear matrix inequalities in control. *Lecture Notes in Dutch Institute for Systems and Control*. Delft. The Netherlands. 2000; 3.
- Kemer E, Başak H, Prempain E. Switched H_2 -state-feedback control with application to a fighter aircraft. *Proceedings of the Institution of Mechanical Engineers, Part G: Journal of Aerospace Engineering*. 2019; 233(14): 5428-5437.
- Richter H. *Advanced control of turbofan engines*. Springer Science & Business Media; 2011.
- Jaw L, Mattingly J. *Aircraft engine controls: Design, System Analysis and Health Monitoring*. Reston VA. USA: American Institute of Aeronautics and Astronautics; 2009.

Emre Kemer:  <https://orcid.org/0000-0001-8716-1971>

Hasan Başak:  <https://orcid.org/0000-0002-3724-6819>



This work is licensed under the Creative Commons BY-NC-ND 4.0 license.